

## Self-irradiation enhanced tritium solubility in hydrogenated amorphous and crystalline silicon

Baojun Liu, Kevin P. Chen, Nazir P. Kherani, Tome Kostascki, Keith R. Leong, and Stefan Zukotynski

Citation: *Journal of Applied Physics* **109**, 054902 (2011); doi: 10.1063/1.3549145

View online: <http://dx.doi.org/10.1063/1.3549145>

View Table of Contents: <http://scitation.aip.org/content/aip/journal/jap/109/5?ver=pdfcov>

Published by the [AIP Publishing](#)

---

### Articles you may be interested in

[Damage at hydrogenated amorphous/crystalline silicon interfaces by indium tin oxide overlayer sputtering](#)  
*Appl. Phys. Lett.* **101**, 171604 (2012); 10.1063/1.4764529

[Critical oxygen concentration in hydrogenated amorphous silicon solar cells dependent on the contamination source](#)

*Appl. Phys. Lett.* **96**, 103505 (2010); 10.1063/1.3357424

[Thermal activation energy for the passivation of the n -type crystalline silicon surface by hydrogenated amorphous silicon](#)

*Appl. Phys. Lett.* **94**, 162102 (2009); 10.1063/1.3120765

[Room temperature ferromagnetism in Cr-doped hydrogenated amorphous Si films](#)

*Appl. Phys. Lett.* **92**, 242501 (2008); 10.1063/1.2946662

[The effect of hydrogen on the network disorder in hydrogenated amorphous silicon](#)

*Appl. Phys. Lett.* **75**, 2803 (1999); 10.1063/1.125155

---



**2014 Special Topics**

PEROVSKITES

2D MATERIALS

MESOPOROUS MATERIALS

BIOMATERIALS/ BIOELECTRONICS

METAL-ORGANIC FRAMEWORK MATERIALS

**AIP** | APL Materials

**Submit Today!**

## Self-irradiation enhanced tritium solubility in hydrogenated amorphous and crystalline silicon

Baojun Liu,<sup>1</sup> Kevin P. Chen,<sup>1,a)</sup> Nazir P. Kherani,<sup>2,3</sup> Tome Kostascki,<sup>2</sup> Keith R. Leong,<sup>2</sup> and Stefan Zukotynski<sup>2</sup>

<sup>1</sup>*Department of Electrical and Computer Engineering, University of Pittsburgh, Pittsburgh, Pennsylvania 15261, USA*

<sup>2</sup>*Department of Electrical and Computer Engineering, University of Toronto, Toronto, Ontario M5S 3G4, Canada*

<sup>3</sup>*Department of Materials Science and Engineering, University of Toronto, Toronto, Ontario M5S 3E4, Canada*

(Received 6 October 2010; accepted 13 December 2010; published online 2 March 2011)

Experimental results on tritium effusion, along with the tritium depth profiles, from hydrogenated amorphous silicon (a-Si:H) and crystalline silicon (c-Si) tritiated in tritium ( $T_2$ ) gas at various temperatures and pressures are presented. The results indicate that tritium incorporation is a function of the material microstructure of the as-grown films, rather than the tritium exposure condition. The highest tritium concentration obtained is for a-Si:H deposited at a substrate temperature of 200°C. The tritium content is about 20 at. % on average with a penetration depth of about 50 nm. In contrast, tritium occluded in the c-Si is about 4 at. % with penetration depth of about 10 nm. The tritium concentration observed in a-Si:H and c-Si is much higher than the reported results for the post-hydrogenation process.  $\beta$  irradiation appears to catalyze the tritiation process and enhance tritium dissolution in the silicon matrix. The combination of tritium decay and  $\beta$ -induced ionizations results in formation of reactive species of tritium (tritium atoms, radicals, and ions) that readily adsorb on silicon. The electron bombardment of the silicon surface and subsurface renders it chemically active thereby promoting surface adsorption and subsurface diffusion of tritium, thus leading to tritium occlusion in the silicon matrix. Gaussian deconvolution of tritium effusion spectra yields two peaks for a-Si:H films tritiated at high temperature (250°C), one low temperature (LT) peak which is attributed to tritiated clusters and higher order tritides, and another high temperature peak which is attributed to monotritides. Activation energy of 2.6–4.0 eV for the LT peak was found. © 2011 American Institute of Physics. [doi:10.1063/1.3549145]

### I. INTRODUCTION

With the rapid development of microelectronics and microelectromechanical systems (MEMS) technology, there is increasing interest to develop niche nuclear micropower sources for chip-scale applications.<sup>1–7</sup> Radioactive isotope micropower sources (RIMS) offer a number of unique advantages including its high power density and long operation life. One of the daunting challenges for chip-scale RIMS applications is to develop a safe and cost-effective method of integrating radioactive material on-chip with minimal collateral contamination to surrounding microelectronics circuits or MEMS structures. It is also important that the process to integrate radioactive materials on-chip should be compatible with existing microfabrication processes with minimal radiation cross-contamination to the fabrication facilities.

Tritium ( $T$ ,  $^3H$ ), the radioactive isotope of hydrogen, is one of the best candidates for chip-scale RIMS from nW to  $\mu W$  level.<sup>6–13</sup> As a by-product of many nuclear power plants, tritium is plentiful and available at relatively low cost. It is a pure  $\beta$  emitter with benign radiation and moderate half-life of 12.3 years. The potential radiation health hazard is

minimal. To integrate high-density tritium fuel on-chip for battery applications, a dc saddle field plasma enhanced chemical vapor deposition (PECVD) technique has been used to incorporate tritium into hydrogenated amorphous silicon (a-Si:H).<sup>8,14,15</sup> In recent years the incorporation of high-density tritium into amorphous and crystalline silicon material using a post-tritiation technique has been reported. Here silicon following its synthesis was tritiated by directly exposing it to tritium gas ( $T_2$ ) at elevated temperature.<sup>12,15</sup> These studies suggest that tritium can be readily and locally integrated on-chip using a “post-process” tritiation procedure, for example, implemented after the fabrication of MEMS and microelectrical devices, and thus offering a clean and versatile method to integrate radioactive fuel on-chip.

Different from other post-hydrogenation processes which involve monoatomic hydrogen or hydrogen plasma,<sup>12</sup> the reported post-tritiation process uses pressurized tritium gas in the molecular form. Although it is commonly believed that hydrogen molecules are chemically inactive to silicon, high concentration of tritium incorporation was observed. The unique radioactive property of tritium appears to catalyze the tritiation process.

In this paper, we report the thermal effusion and tritium depth profile results in both tritiated crystalline and amorphous silicon obtained by the post-tritiation process. In

<sup>a)</sup>Author to whom correspondence should be addressed. Electronic mail: kchen@enr.pitt.edu.

contrast to the relatively large quantity of literature on the effect of post-hydrogenation and post-deuteration,<sup>16</sup> almost no study has involved post-tritiation of amorphous and crystalline silicon. These studies aim to clarify the post-tritiation mechanism between tritium gas and silicon materials. From an engineering perspective, this study will provide useful information on how tritium post-processing and tritium-based nuclear microengineering can impact silicon microelectronics on-chip.

Using the radiotracer property of tritium, effusion measurements were used to characterize the concentration, thermal stability, and bonding characteristics of tritium in crystalline silicon (c-Si) and hydrogenated amorphous silicon (a-Si:H) deposited and tritiated under different conditions.<sup>2,17,18</sup> The bonding and structural characteristics of tritium in silicon were characterized using thermal effusion measurement. The free energy of tritium desorption in the tritiated silicon is estimated. Tritium concentration and depth profile was also measured using secondary ion mass spectroscopy (SIMS). Tritium dissolution and permeation in amorphous and crystalline silicon under the influence of tritium decay induced irradiation is characterized and discussed.

## II. EXPERIMENTAL

The a-Si:H films were deposited on crystalline silicon substrates using a dc saddle-field glow discharge PECVD system which has been described elsewhere.<sup>8,14,17</sup> The precursor gas used in the depositions was silane (SiH<sub>4</sub>). The depositions reported here involved the flow of pure silane gas through the glow discharge chamber at 15 sccm at a chamber pressure of 160 mTorr, anode potential of 530–650 V, current to the anode of 17.5 mA, substrate at ground potential, and ion current to substrate of 0.6–1.0 mA. The substrate temperature, duration of the deposition, thickness of the film and hydrogen concentration of the a-Si:H films are listed in Table I.

In order to test for tritium permeation into the different silicon samples, the samples were exposed to tritium gas at temperatures of 100–250°C and pressures of 2–120 bar for durations of 20 to 132 h. The tritium loading system has been described elsewhere.<sup>11,19</sup>

Tritium effusion experiments were conducted in order to determine the atomic concentration in the samples and its bonding characteristics.<sup>17,18</sup> The detailed experimental setup and procedure have been described previously<sup>17,18</sup> and is briefly described here. The sample was mounted in a 1 L ionization chamber which was purged and then filled with argon gas at 800 Torr. Tritiated samples were heated from room

temperature to 800°C at linear ramp rates of 10 or 20 K/min. The tritium, released from the samples undergoes  $\beta$  decay, the energetic  $\beta$  particles in turn ionize the argon gas, and the ion pairs are separated by virtue of an electrical field due to a potential difference between the cylindrical collector and the concentric outer ionization chamber wall. The electrical field is sufficiently strong that all the ions are collected and consequently the collector current is directly proportional to the number of tritium atoms in the ion chamber. The time derivative of the collector current is directly proportional to the rate of tritium effusion. The collector current is monitored as a function of time using computer-aided data acquisition system. The tritium effusion chamber has a sensitivity of 1  $\mu$ Ci.

Time-of-flight secondary ion mass spectroscopy (SIMS) measurements were carried out to determine the depth profile of tritium in the silicon samples using Cs<sup>+</sup> sources. Given the total atomic concentrations for the samples as determined by the effusion measurements, the SIMS profiles were carefully quantified. The depth resolution of SIMS profiling is  $\sim$ 0.1 nm. The diffusion coefficient of tritium was derived from the tritium concentration profiles.

## III. RESULTS

### A. Tritium contents

The a-Si:H samples deposited under different conditions were exposed to tritium gas for 84 h at a temperature of 250°C and a pressure of 120 bar. Thermal effusion measurements were then carried out to determine the tritium concentration and bonding characteristics. Similar profiles are observed for all three samples deposited under different conditions. Figures 1(a) and 1(b) show the tritium effusion profile and tritium evolution rate as a function of temperature for samples a-Si:H1 and a-Si:H3. The effusion profile for a-Si:H2 can be found in Ref. 11. The profiles show that tritium begins to effuse significantly above a loading temperature of 250°C and that most of the tritium is effused below 700°C. Gaussian deconvolution was employed to analyze the tritium evolution rate profile. Table II lists the positions of the two peaks and the corresponding fractional areas of the tritium effusion peaks for all three tritiated a-Si:H samples. For all three samples, the low-temperature (LT) peak is located around 370°C and the high temperature (HT) peak is centered around 500°C, which agrees with previous effusion studies on tritiated hydrogenated amorphous silicon (a-Si:H:T) prepared by the PECVD process.<sup>2,17,18</sup> The LT peaks suggest the existence of high order silicon tritides and tritium clusters, and the HT peak could be attributed predominantly to the Si–T monotrityde bonds.<sup>12,17</sup> By comparing the fractional areas under both HT and LT peaks, it is estimated that around 70% of the tritium in a-Si:H films exists in the form of high order silicon tritides and tritium cluster. Despite identical tritium loading conditions and similar effusion profiles, the tritium concentrations in the three samples are significantly different. The effusion measurement yielded tritium activities of 1.2, 3.3, and 0.6 mCi/cm<sup>2</sup> for samples a-Si:H1, a-Si:H2, and a-Si:H3, respectively. Those values are the measured tritium content normalized to the area of the samples. The error range is around 0.02 mCi/cm<sup>2</sup>; this is

TABLE I. Substrate temperature, time duration of the deposition, thickness, and hydrogen concentration in the a-Si:H films.

Sample	Substrate temperature (°C)	Duration of deposition (h)	Thickness of film ( $\mu$ m)	Hydrogen concentration (%)
a-Si:H1	115	5.25	0.6	35
a-Si:H2	200	3	0.3	20
a-Si:H3	315	5	2.0	17

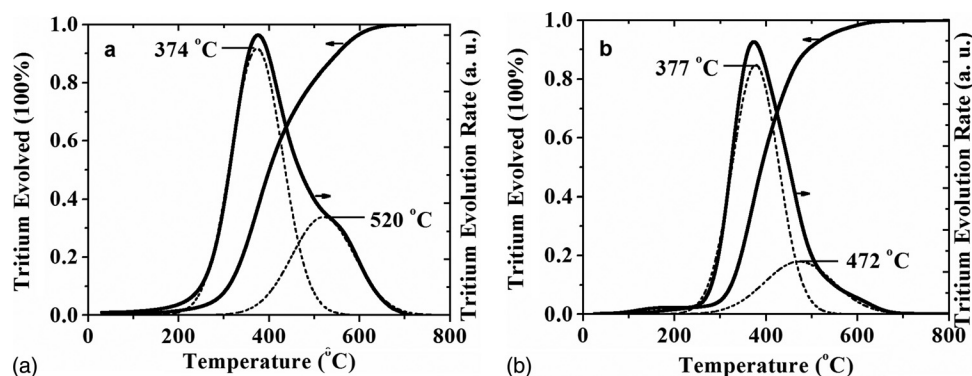


FIG. 1. Total tritium effusion from tritiated a-Si:H films, and tritium effusion rate as a function of temperature for samples (a) a-Si:H1 and (b) a-Si:H3. The samples were tritiated in tritium gas for 84 h at a temperature of 250°C and a pressure of 120 bar. The Gaussian deconvolutions of the tritium evolution rates are shown as dashed curves.

associated with the sensitivity of the effusion monitor. The a-Si:H film that was deposited at 200°C yields the highest tritium concentration upon tritium exposure. The film deposited above 300°C will have a tighter lattice structure which will effectively hinder the permeation of hydrogen. The large concentration of hydrogen in the film that was deposited at low temperature upon tritium exposure also results in lower absorption of tritium; this suggests that the high hydrogen concentration in the as-deposited a-Si:H films has a negative impact on the tritiation process, and that the isotope exchange process between H and T is not significant.

To study the influence of tritiation temperature and pressure on tritium incorporation, sample a-Si:H2 was exposed to T<sub>2</sub> gas under two different conditions: temperature at 100°C with pressure of 70 bar, and temperature at 70°C with pressure of 2 bar. The exposure time was 84 h, identical to the above described exposure at 250°C. The former condition yielded a tritium activity of 3.1 mCi/cm<sup>2</sup> and the latter 3.3 mCi/cm<sup>2</sup>. Despite dramatically different exposure conditions, there is no significant difference in the total tritium absorbed in the film under different tritium pressure and temperature. The results suggest that the tritium incorporation in a-Si:H is predominately determined by the material microstructures, which are defined by the deposition condition.

To further study the relation between the tritium permeation and the material structure, sample a-Si:H3 was thermally annealed and subjected to the tritium exposure at the previously used condition: 250°C, 120 bar, and 84 h. The annealing was performed in argon gas at 400°C for 24 h and it reduced the hydrogen concentration from 17 to 6 at. %. Commercially available 500- $\mu$ m thick c-Si wafer is used

TABLE II. Tritium concentration, position of low temperature, and high temperature peaks obtained by Gaussian deconvolution, fractional areas of the peaks, and the free energy of desorption for films a-Si:H1, a-Si:H2, and a-Si:H3 which were tritiated in tritium gas for 84 h at a temperature of 250°C and a pressure of 120 bar.

Sample	Tritium concentration (mCi/cm <sup>2</sup> ) <sup>a</sup>	T (°C) LT peak <sup>b</sup>	T (°C) HT peak <sup>b</sup>	A <sub>LT</sub> /A <sub>T</sub> <sup>c</sup>	A <sub>HT</sub> /A <sub>T</sub>
a-Si:H1	1.2	374	520	0.68	0.32
a-Si:H2	2.8	370	500	0.74	0.26
a-Si:H3	0.6	377	472	0.76	0.24

<sup>a</sup>The error range is  $\pm 0.02$  mCi/cm<sup>2</sup>.

<sup>b</sup>LT: low temperature; HT: high temperature.

<sup>c</sup>A<sub>T</sub>: Total area under the peaks.

here as a reference with extremely tight lattice and no hydrogen content. Tritium effusion profile of annealed a-Si:H3 is shown in Fig. 2. The annealed a-Si:H3 absorbed slightly more tritium than the unannealed sample. This is attributed to a relatively higher dangling bond density notwithstanding the annealing. The effusion peak for the annealed sample shifts to a higher temperature and the fractional area under the high temperature peak increases accordingly. This suggests an increased portion of tritium existing in the Si-T monitride form. Annealing is known to cause densification of the amorphous film and hence a tighter lattice configuration; thus, this process is expected to suppress the formation of tritium clusters in matrix. The tritium concentration, position of low temperature and high temperature peaks yielded by Gaussian deconvolution, fractional areas of the peaks for the annealed a-Si:H3 and c-Si are summarized in Table III. As an example of an extreme situation, tritium occlusion in c-Si is dominated by stably bonded monitrides as shown in Table III. The effusion profile of tritiated c-Si was reported in Ref. 11.

## B. Tritium depth profiles

To study tritium diffusion profiles, SIMS measurements were performed on both tritiated a-Si:H and c-Si. Tritium concentration profiles of sample a-Si:H2 for hydrogen (H), tritium (T), and the total concentration of hydrogen and

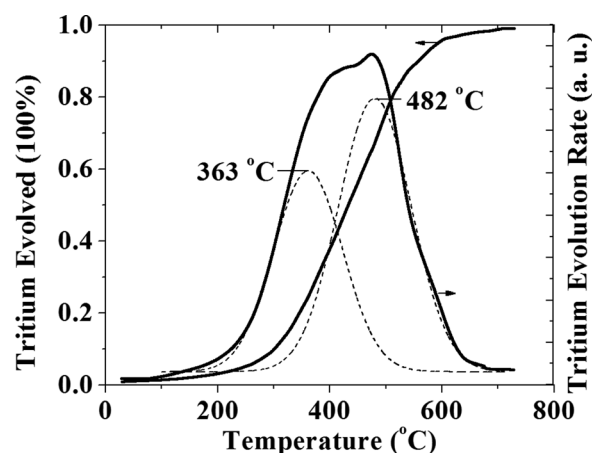


FIG. 2. Tritium effusion and tritium effusion rate as a function of temperature, as well as the Gaussian deconvolution, for the sample a-Si:H3 which was annealed at 400°C (denoted annealed a-Si:H3') and then tritiated in tritium gas for 84 h at a temperature of 250°C and a pressure of 120 bar.



TABLE III. Tritium concentration, position of low temperature, and high temperature peaks yielded by Gaussian deconvolution, and fractional areas of the peaks for samples of annealed a-Si:H3 and c-Si both of which were tritiated in tritium gas for 84 h at a temperature of 250°C and a pressure of 120 bar.

Sample	Tritium concentration (mCi/cm <sup>2</sup> )	T (°C) LT peak	T (°C) HT peak	A <sub>LT</sub> /A <sub>t</sub>	A <sub>HT</sub> /A <sub>t</sub>
annealed a-Si:H3	0.8 <sup>a</sup>	363	482	0.41	0.59
c-Si	0.1 <sup>b</sup>	374	482	0.15	0.85

<sup>a</sup> The error range is  $\pm 0.02$  mCi/cm<sup>2</sup>.

<sup>b</sup> The error range is  $\pm 0.005$  mCi/cm<sup>2</sup>.

tritium (H+T) are shown in Fig. 3. The a-Si:H was exposed to T<sub>2</sub> gas at 250°C, 120 bar for 84 h. The tritiated sample had been stored for three months before the SIMS measurement was performed. There is outgassing associated tritium concentration drop near the superficial surface. Regardless of the tritium drop at the top layers of the film, an extremely tritium-rich layer forms near the surface as observed in the figure, the tritium concentration reaches  $7 \times 10^{22}$  cm<sup>-3</sup> at a depth of 3 nm from the surface, which suggests a large portion of dihydride content near the surface. The concentration drops rapidly while moving inwards reaching approximately  $3 \times 10^{22}$  cm<sup>-3</sup> at a depth of about 6 nm. The tritium concentration then falls off at a slower rate into the sample. Significant hydrogen loss is observed near the surface. At a depth of 6 nm, the hydrogen concentration drops to about  $3 \times 10^{21}$  cm<sup>-3</sup>, which is about 30% of the hydrogen concentration ( $10^{22}$  cm<sup>-3</sup>) in the untritiated sample. The loss of H is attributed to possible isotopic exchange owing to the very high tritium pressure during tritium charging of the sample. The total concentration of hydrogen and tritium is around  $2 \times 10^{22}$  cm<sup>-3</sup> at a depth of 6 nm from the surface. From this depth inwards, the concentration profiles are observed to drop monotonically, and accordingly the diffusion profile can be described by a complementary error function. The diffusion length is related to the diffusion time  $t_d$  by<sup>20</sup>

$$x_0 = (4D_{\text{eff}}t_d)^{1/2}. \quad (1)$$

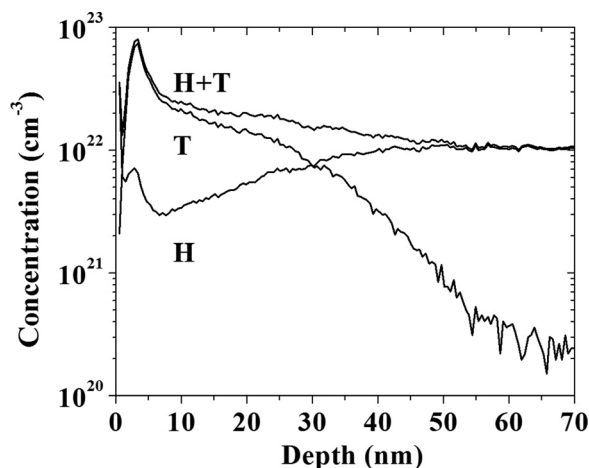


FIG. 3. Hydrogen and tritium depth profiles of tritiated a-Si:H2 obtained after an exposure to T<sub>2</sub> gas at 250°C and 120 bar for 84 h. The concentration profiles for H and T were measured simultaneously.

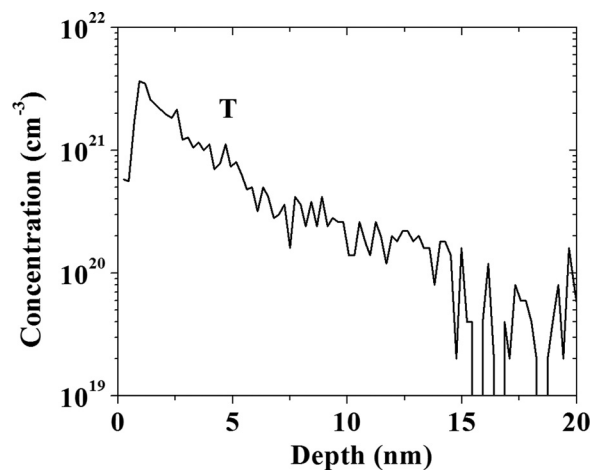


FIG. 4. Tritium depth profiles of crystalline silicon obtained after an exposure to T<sub>2</sub> gas at 250°C and 100 bar for 132 h.

The diffusion length for T in-diffusion is approximately 50 nm ( $x_0$ ). Therefore, a diffusion coefficient of  $D_{\text{eff}} = 6 \times 10^{-17}$  cm<sup>2</sup>/s is inferred. This value is consistent with the reported result of plasma in-diffusion in a-Si:H.<sup>16</sup>

Figure 4 shows the hydrogen and tritium profiles of c-Si tritiated in tritium gas of 250°C and 100 bar for 132 h. The tritiated sample had been stored for three months when the SIMS was performed. A tritium concentration of 8 at. % and a number density of  $4 \times 10^{21}$  cm<sup>-3</sup>, is observed near the surface followed by a rapid drop in concentration with depth. The concentration drops to 1/10 of the surface concentration at a depth of  $\sim 5$  nm. The diffusion coefficient is calculated to be  $D_{\text{eff}} = 5 \times 10^{-19}$  cm<sup>2</sup>/s. Clearly, tritium is located at the superficial surface of c-Si, the tight lattice of the crystalline silicon preventing in-depth tritium permeation.

## IV. DISCUSSION

### A. Tritium solubility

In the reported literature, studies of hydrogen solubility in a-Si:H have been performed using rich deuterium (D) source layer diffusion or post-hydrogenation/deuteration with plasma/monoatomic hydrogen treatment or ion implantation.<sup>16,21–23</sup> In the D diffusion and plasma/monoatomic hydrogen treatment, hydrogen solubility of 1–3% has been observed.<sup>22,24</sup> At such low concentration levels, the weak Si–Si bonds and dangling bonds seem to provide sites for H incorporation without dilation of the silicon network; the solubility depends on the microstructure which, in turn, depends on the deposition conditions for the film. In the ion implantation process, the hydrogen incorporation proceeds simultaneously with defect creation, hence a higher H concentration can be achieved than the initial H concentration. A hydrogen solubility limit of about 15–16% was reported in a-Si:H prepared by PECVD.<sup>25</sup> In this work, a much higher tritium concentration is observed from SIMS measurement. Ignoring the ultrahigh tritium concentration layer near the surface, a stabilized tritium concentration of  $3 \times 10^{22}$  cm<sup>-3</sup> is attained, which is equivalent to a tritium to silicon ratio of 3:5. This differs significantly from the previously reported results from post-hydrogenation and post-deuteration. Apparently,

here there are more Si bonds broken and more space provided for far more tritium accommodation. Given the radioactive property of tritium, the solubility of tritium in silicon is enhanced by  $\beta$  irradiation. Two effects are expected to occur due to  $\beta$  radiation. (i) The tritium decay induced ionizations result in the formation of reactive species of tritium (tritium atoms, radicals, and ions) that readily adsorb on silicon. (ii) Electron bombardment of the silicon surface and subsurface is expected to render it chemically active thereby promoting surface adsorption and subsurface diffusion of tritium, thus leading to tritium occlusion in the silicon matrix.

In the tritium exposure system, there is about 1 cm thick gaseous T<sub>2</sub> layer above the silicon sample.  $\beta$  particles emitted from tritium decay can travel up to 35 mm in tritium gas at one atmosphere. The average range of the  $\beta$  particles in silicon decreases with increase in tritium pressure. For pressurized tritium gas, the electron flux will saturate at about  $\phi = 5 \times 10^{11} \text{ cm}^{-2} \text{ s}^{-1}$ .<sup>1,6</sup> The electron bombardment excites the silicon surface and makes it chemically active to the ionized or dissociated tritium. Thus, tritium can be absorbed at the sample surface. The  $\beta$  radiation is also likely to provide more positions for tritium in the silicon material. For the  $\beta$  particles impinging the material, they lose energy in collision with the electrons in the material and produce an extremely large density of electron-hole pairs (EHPs) in their tracks. In case of a-Si:H, a pair is created for every 4.3 eV.<sup>26</sup> Electrons of 5.7 keV can produce about 1300 pairs. The electron hole recombination can in turn break Si-H bonds to produce mobile H and DBs (dangling bonds).<sup>27</sup> While traversing the matrix, the  $\beta$  particles lose energy rapidly with depth and the effective active depth for electrons with energy of  $\sim 5.7$  keV is around 50 nm in a-Si:H.<sup>28</sup> Within this depth, extra DBs will be created and provide for the hydrogen (tritium) accommodation. This is consistent with the tritium depth observed in Fig. 3.

From the above analysis,  $\beta$  irradiation due to tritium is likely the reason for the very high tritium absorption in a-Si:H. To confirm this, a control experiment was performed. Amorphous silicon was thermally evaporated onto the c-Si substrate with a thickness of 400 nm; amorphous silicon prepared in this way is defect rich and expected to readily absorb hydrogen. The sample was then exposed to high pressure hydrogen gas for 2 weeks at room temperature. The initial pressure was 95 bar and it dropped to 15 bar in 2 weeks due to leakage. Fourier transform infrared spectra of the film before and after the hydrogen loading are shown in Fig. 5. The inset shows the pressure vs time duration for the exposure. A hydrogen concentration of 2.5% was found for the film before the loading and no observable increase of hydrogen content after the high pressure hydrogen exposure after 2 weeks. This result suggests that nonradioactive molecular hydrogen can hardly permeate amorphous silicon.

## B. Free energy of desorption

The Gaussian deconvolution of the effusion rate profiles illustrate two peaks, one low temperature peak and one high temperature peak. The low temperature (LT) peak is around

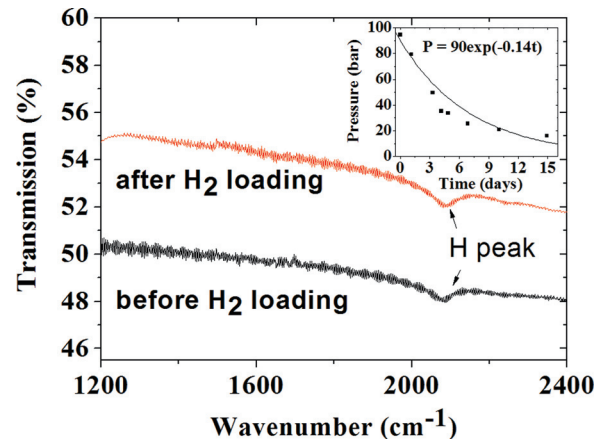


FIG. 5. (Color online) Transmission spectra of amorphous silicon prepared by thermal evaporation on crystalline silicon substrate before and after high pressure hydrogen gas loading. The upper spectrum has been shifted by 0.05 for clarity of presentation. The inset shows the pressure as a function of time during of hydrogen loading.

370°C and the high temperature (HT) one around 500°C. The low temperature hydrogen effusion is usually considered to be limited by surface desorption process, which can be represented by the following surface desorption rate equation:<sup>18,29–31</sup>

$$\frac{d\left(\frac{N}{N_0}\right)}{dt} = \left(\frac{kT}{h}\right) \left[1 - \left(\frac{N}{N_0}\right)\right]^n \exp\left(-\frac{\Delta G}{kT}\right), \quad (2)$$

where  $N$  and  $N_0$  represent the hydrogen evolved from the sample and the initial hydrogen in the sample, respectively,  $T$  is the sample temperature,  $n$  is the reaction order which is 1 or 2, and  $\Delta G$  is the free energy of desorption. Applying this rate equation to the LT peaks by plotting

$$\ln \left\{ \left[ \frac{d\left(\frac{N}{N_0}\right)}{dt} \right] \left(\frac{kT}{h}\right)^{-1} \left(1 - \frac{N}{N_0}\right)^{-n} \right\}$$

as a function of  $1/T$  results in a straight line for  $n=1$ , which indicates that the desorption reaction is a first order reaction process. The calculated free energies for a-Si:H1, a-Si:H2, a-Si:H3, and annealed a-Si:H3, all samples having been tritiated at 250°C, 120 bar, and 84 h, are calculated to be 3.0, 2.6, 4.0, and 4.0 eV, respectively. The surface absorption of hydrogen involves the simultaneous rupture of two neighboring Si-H bonds and formation of H<sub>2</sub>. Considering the hydrogen bonding energy  $E_{\text{H-H}}$  of 4.5 eV, the silicon-tritium bond energy is calculated to be 3.55–4.25 eV. This is generally in agreement with the literature data.<sup>16</sup> Here, the mass difference between hydrogen and tritium is neglected. The range of energies suggests variation in the Si-T bonding environment. Higher activation energy of 4.0 eV is obtained for tritiated a-Si:H films deposited or annealed at high temperature (300–400°C); in comparison, lower activation energy is found for films deposited at low temperature (100–200°C). This suggests that the film morphology affects the tritium bonding in the post-tritiation process.

## V. CONCLUSIONS

Tritium effusion and SIMS techniques are employed to study tritium evolution from a-Si:H films deposited and tritiated under various conditions, as well as tritiated c-Si. The results indicate that the tritium incorporation is determined mainly by the material microstructure which depends on the deposition conditions. Gaussian deconvolution of tritium effusion spectra yield two peaks for a-Si:H films, which were tritiated at high temperature (250°C): One low temperature (LT) peak which is attributed to tritium clusters and weakly bonded tritium and another high temperature (HT) peak which is attributed to monotritides. The activation energy of 2.6–4.0 eV for the LT peak was derived. The Si-H bond energies range from 3.55–4.25 eV. Due to a much tighter lattice, c-Si absorbed less tritium than a-Si:H. The concentration near the surface is 40 and 8% in a-Si:H and c-Si, respectively. This is much higher than the reported results from post-hydrogenation and post-deuteriation studies. The solubility is enhanced by the electron bombardment due to  $\beta$ -decay of tritium. The high energy electrons effectively makes the material surface chemically active, promoting  $\beta$  induced tritium-material interactions.

## ACKNOWLEDGMENTS

This work was supported by NSF Grant No. 0826289 and NSERC discovery grants. The authors wish to thank Dr. Armando B. Antoniazzi and Mr. Clive Morton for their assistance in tritium loading. The help in preparation of the a-Si:H samples from Dr. D. Yeghikyan is also gratefully acknowledged.

<sup>1</sup>K. E. Bower, Y. A. Barbanel, Y. G. Shreter, and G. W. Bohnert, *Polymer, Phosphors, and Volatiles for Radioisotope Microbatteries* (CRC Press, Boca Raton, FL, 2002).

<sup>2</sup>T. Kostascki, N. P. Kherani, P. Stradins, F. Gaspari, W. T. Shmayda, L. S. Sidhu, and S. Zukotynski, *IEE Proc.: Circuits Devices Syst.* **150**(4), 274 (2003).

<sup>3</sup>A. Lal and J. Blanchar, *IEEE Spectrum* **41**(9), 36 (2004).

<sup>4</sup>W. Sun, N. P. Kherani, K. D. Hirschman, L. L. Gadeken, and P. M. Fauchet, *Adv. Mater. (Weinheim, Ger.)* **17**(10), 1230 (2005).

<sup>5</sup>M. V. S. Chandrashekhar, C. I. Thomas, H. Li, M. G. Spencer, and A. Lal, *Appl. Phys. Lett.* **88**(3), 033506 (2006).

<sup>6</sup>B. Liu, K. P. Chen, N. P. Kherani, and S. Zukotynski, *Appl. Phys. Lett.* **95**(23), 233112 (2009).

<sup>7</sup>B. Liu, K. P. Chen, N. P. Kherani, S. Zukotynski, and A. B. Antoniazzi, *Appl. Phys. Lett.* **92**(8), 083511 (2008).

<sup>8</sup>T. Kostascki, N. P. Kherani, F. Gaspari, S. Zukotynski, and W. T. Shmayda, *J. Vac. Sci. Technol. A* **16**(2), 893 (1998).

<sup>9</sup>B. Liu, N. P. Kherani, K. P. Chen, and S. Zukotynski, *Fusion Sci. Technol.* **54**, 627 (2008).

<sup>10</sup>B. Liu, N. P. Kherani, S. Zukotynski, and K. P. Chen, in *Conference on Lasers and Electro-Optics/Quantum Electronics and Laser Science Conference and Photonic Applications Systems Technologies* (Technical Digest, Optical Society of America, Long Beach, CA, 2006).

<sup>11</sup>B. Liu, K. P. Chen, N. P. Kherani, S. Zukotynski, and A. B. Antoniazzi, *Appl. Phys. Lett.* **88**(13), 134101 (2006).

<sup>12</sup>B. Liu, K. P. Chen, N. P. Kherani, T. Kostascki, S. Costea, S. Zukotynski, and A. B. Antoniazzi, *Appl. Phys. Lett.* **89**(4), 044104 (2006).

<sup>13</sup>B. Liu, F. Yan, U. Phillipose, N. P. Kherani, W. Shmayda, H. Ruda, and K. P. Chen, *J. Phys. D* **43**(41), 415502 (2010).

<sup>14</sup>N. P. Kherani, T. Kostascki, S. Zukotynski, and W. T. Shmayda, *Fusion Technol.* **28**(3), 1609 (1995).

<sup>15</sup>B. Liu, D. Alvarez-Ossa, N. P. Kherani, S. Zukotynski, and K. P. Chen, *IEEE Sens. J.* **7**, 917 (2007).

<sup>16</sup>W. Beyer, *Sol. Energy Mater. Sol. Cells* **78**(1–4), 235 (2003).

<sup>17</sup>T. Kostascki, Ph.D thesis, University of Toronto, 2001.

<sup>18</sup>N. P. Kherani, B. Liu, K. Virk, T. Kostascki, F. Gaspari, W. T. Shmayda, S. Zukotynski, and K. P. Chen, *J. Appl. Phys.* **103**(2), 024906 (2008).

<sup>19</sup>A. B. Antoniazzi, C. S. Morton, K. P. Chen, and B. Liu, *Fusion Sci. Technol.* **54**(2), 635 (2008).

<sup>20</sup>B. Tuck, *Introduction to Diffusion in Semiconductors* (Peregrinus, Salisbury, 1974).

<sup>21</sup>N. H. Nickel and W. B. Jackson, *Phys. Rev. B* **51**(8), 4872 (1995).

<sup>22</sup>W. B. Jackson and C. C. Tsai, *Phys. Rev. B* **45**(12), 6564 (1992).

<sup>23</sup>J. Pearton, J. W. Corbett, and M. Stavola, *Hydrogen in Crystalline Semiconductors*. (Springer-Verlag, New York, 1992).

<sup>24</sup>S. Acco, D. L. Williamson, P. A. Stolk, F. W. Saris, M. J. vandenBoogaard, W. C. Sinke, W. F. vanderWeg, and S. Roorda, *Phys. Rev. B* **53**(8), 4415 (1996).

<sup>25</sup>P. Danesh, B. Pantchev, B. Schmidt, and D. Grambole, *Semicond. Sci. Technol.* **19**, 1422 (2004).

<sup>26</sup>J. Dubeau, L. A. Hamel, and T. Pochet, *Phys. Rev. B* **53**(16), 10740 (1996).

<sup>27</sup>A. Yelon, H. Fritzsche, and H. M. Branz, *J. Non-Cryst. Solids* **266**, 437 (2000).

<sup>28</sup>S. Najjar, B. Equer, and N. Lakhoua, *J. Appl. Phys.* **69**(7), 3975 (1991).

<sup>29</sup>J. A. Mcmillan and E. M. Peterson, *J. Appl. Phys.* **50**(8), 5238 (1979).

<sup>30</sup>W. Beyer and H. Wagner, *J. Appl. Phys.* **53**(12), 8745 (1982).

<sup>31</sup>W. Beyer, *Physica B* **170** (1–4), 105 (1991).